Environmental Pollution 311 (2022) 119981

Contents lists available at ScienceDirect

Environmental Pollution

journal homepage: www.elsevier.com/locate/envpol

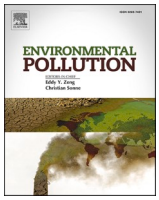

Long-distance transport of per- and polyfluoroalkyl substances (PFAS) in a Swedish drinking water aquifer☆

Mattias Sörengård [a], Sofia Bergström [a], Philip McCleaf [b], Karin Wiberg [a], Lutz Ahrens [a,*]

[a] Department of Aquatic Sciences and Assessment, Swedish University of Agricultural Sciences (SLU), P.O. Box 7050, SE-750 07, Uppsala, Sweden
[b] Uppsala Water and Waste Ltd., P.O. Box 1444, SE-751 44, Uppsala, Sweden

ARTICLE INFO

Keywords:
PFAS
PFOS
AFFF
Soil
Groundwater
Drinking water

ABSTRACT

Use of per- and polyfluoroalkyl substance (PFAS)-containing aqueous film-forming foams (AFFF) at firefighting training sites (FFTS) has been linked to PFAS contamination of drinking water. This study investigated PFAS transport and distribution in an urban groundwater aquifer used for drinking water production that has been affected by PFAS-containing AFFF. Soil, sediment, surface water and drinking water were sampled. In soil (n = 12) at a FFTS with high perfluorooctane sulfonate (PFOS) content (87% of ∑PFAS), the ∑PFAS concentration (n = 26) ranged from below detection limit to 560 ng g^{-1} dry weight. In groundwater (n = 28), the ∑PFAS concentration near a military airbase FFTS reached 1000 ng L^{-1}. Principal component analysis (PCA) identified the military FFTS as the main source of PFAS contamination in drinking water wellfields >10 km down-gradient. Groundwater samples taken close to the military FFTS site showed no ∑PFAS concentration change between 2013 and 2021, while a location further down-gradient showed a transitory 99.6% decrease. Correlation analysis on PFAS composition profile indicated that this decrease was likely caused by dilution from an adjacent conflating aquifer. ∑PFAS concentration reached 15 ng L^{-1} (PFOS 47% and PFHxS 41% of ∑PFAS) in surface river water (n = 6) and ranged between 1 ng L^{-1} and 8 ng L^{-1} (PFHxS 73% and PFBS 17% of ∑PFAS) in drinking water (n = 4). Drinking water had lower PFAS concentrations than the wellfields due to PFAS removal at the water treatment plant. This demonstrates the importance of monitoring PFAS concentrations throughout a groundwater aquifer, to better understand variations in transport from contamination sources and resulting impacts on PFAS concentrations in drinking water extraction areas.

1. Introduction

There is increasing concern about per- and polyfluoroalkyl substances (PFAS), a group of highly fluorinated synthetic organic compounds comprising >4700 unique species recorded by the OECD (OECD, 2018; Chelcea et al., 2020). Their surfactant-like, water- and oil-repellent properties and high chemical stability (Buck et al., 2011; Martin et al., 2019) have led to their use in a wide variety of consumer products and industrial processes (Herzke et al., 2012; Schultes et al., 2018). They have therefore been produced in large quantities for over half a century (Lim et al., 2011; Wang et al., 2017). However, multiple PFAS have been shown to be persistent and non-susceptible to natural degradation (Lemal, 2004; Merino et al., 2016), resulting in bioaccumulation in biota (Pan et al., 2014; Rich et al., 2015) and associated adverse health effects (DeWitt, 2015; Schrenk et al., 2020). As a consequence, PFAS are increasingly regulated, e.g. by the Stockholm Convention on Persistent Organic Pollutants (POPs) (2018). A major exposure pathway for humans is through food and drinking water (European Food Safety Authority EFSA, 2012). Drinking water providers world-wide have been compelled to close PFAS-contaminated wells and in some cases find alternative sources of drinking water, e.g. in Sweden (Li et al., 2018), Japan (Murakami et al., 2009) and Germany (Gellrich et al., 2013). Firefighting training sites (FFTS) (Guelfo and Higgins, 2013; Houtz et al., 2013; Filipovic et al., 2015a), industrial areas (Lin et al., 2009), wastewater treatment plants (WWTPs) (Houtz et al., 2016) and landfill sites (Busch et al., 2010; Benskin et al., 2012) are known to be key sources of PFAS to the environment such as drinking water source areas. Historically, use of aqueous film-forming foams (AFFF) at FFTS on municipal airport and military facilities has led to contamination of adjacent soil and groundwater (Ahrens et al., 2015; Baduel et al., 2015;

☆ This paper has been recommended for acceptance by Hefa Cheng.

* Corresponding author.
E-mail address: Lutz.ahrens@slu.se (L. Ahrens).

https://doi.org/10.1016/j.envpol.2022.119981
Received 26 April 2022; Received in revised form 10 August 2022; Accepted 12 August 2022
Available online 18 August 2022

Filipovic et al., 2015b; Milley et al., 2018). Ionisable PFAS are water-soluble and are known to be released from soil and transported to adjacent surface waters (Place and Field, 2012) and groundwater (Hale et al., 2017; Guo et al., 2020; Sörengård et al., 2020b). However, there is a lack of long-term high-resolution field data on the transport and behaviour of PFAS in groundwater aquifers, which is essential for verifying transport models and improving risk assessment measures.

One known PFAS-polluted site is the groundwater aquifer in Uppsala, Sweden, which supplies approximately 190 000 people with municipal drinking water. PFAS contamination of this aquifer has resulted in elevated blood serum levels in school children (Glynn et al., 2020), young women (Gyllenhammar et al., 2015), first-time mothers (Miaz et al., 2020) and elderly people (Stubleski et al., 2016). Multiple FFTS have been identified in close proximity to the aquifer, wherein the military airbase FFTS located up-gradient from two drinking water wellfields is suspected to be the main point source (Gyllenhammar et al., 2015; Samuelsson and Thorsbrink, 2019). To meet present and future PFAS thresholds for drinking water as established by national and international guidelines (Gobelius et al., 2018), it is imperative to understand the link between PFAS-contaminated FFTS and their impact on PFAS levels in wellfield areas in Uppsala. A clearer understanding of sources and variations in PFAS concentrations in groundwater would facilitate sustainable management of the managed aquifer recharge (MAR) system in Uppsala. This would allow a formulation of a long-term PFAS removal strategy for Bäcklösa drinking water treatment plant (DWTP) (Belkouteb et al., 2020; Franke et al., 2021; McCleaf et al., 2017) and help the local authority identify priority sites for PFAS remediation, e.g. using soil remediation technologies (Ross et al., 2018; Mahinroosta and Senevirathna, 2020).

The overall aim of this study was to provide a holistic understanding of the complex PFAS contamination situation in the groundwater aquifer serving Uppsala, based on determination of PFAS concentration in soil, sediment, groundwater flow, surface water and drinking water. Thereby it is hypothesized that long-term high-resolution field data of PFAS composition profiles can be used to identify sources and exposure pathways. Extensive sampling was performed along the groundwater flow path and in drinking water production wells. The potential source zone was sampled over a period of eight years, which to our knowledge is the largest study to date of an urban groundwater aquifer used for municipal drinking water. Spatial PFAS distribution and compositional profile were analysed to identify point sources at FFTS. Specific objectives of the work were to i) quantify the occurrence of PFAS in an urban groundwater aquifer area; ii) map the unique and complex PFAS transport pathways in the groundwater considering multiple point sources and the hydrogeological system; and iii) perform time-series analysis covering eight years (2013–2021) in order to identify temporal variations in PFAS contamination of the municipal drinking water wellfields, thereby allowing sustainable management of drinking water source areas and reduced human exposure to PFAS.

2. Material and methods

2.1. Study site

The study focused on the urban area of Uppsala, Sweden. Three small eskers (i.e. stratified glaciofluvial sediments of gravel and sand) drain into *Uppsala groundwater aquifer*, namely *Jumskil esker* from the northwest, *Vattholma esker* from the northeast and *Sävja esker* from the southeast. Groundwater flow direction in the *Uppsala groundwater aquifer* is from north to south covering a length of >10 km with the groundwater level approximately +35 m above sea level (MASL) at the aquifer's northern groundwater divide and approximately +1 MASL at the aquifer's low point in the south where groundwater is in contact with Lake Ekoln. The aquifer follows a main north-south fault line reaching depths of up to 150 m and is characterized by a hydraulic conductivity of approximately 10^{-2} to 10^{-3} m s^{-1} with greater conductivity at some locations due to bedrock fracture zones. At sites where esker sediments are exposed at the ground surface north of Uppsala, artificial infiltration basins were established in 1965 as part of the MAR system for Uppsala City's drinking water supply (Winquist, 1992). The City's drinking water has been affected by PFAS contamination of the groundwater, with $\sum_{17}$PFAS concentrations of up to 250 ng L^{-1} (Belkouteb et al., 2020). This exceeds the existing Swedish drinking water guideline value of 90 ng L^{-1} for the sum of 11 PFAS ($\sum_{11}$PFAS) (Swedish Food Agency, 2021) and the European Drinking Water Directive limit of 100 ng L^{-1} considering 20 PFAS (European Commission Directive 98/83/European Commission, 2020).

2.2. Sampling

Samples of soil (n = 12), sediment (n = 2), groundwater (n = 28), surface water (n = 6) and drinking water (n = 4) were collected throughout Uppsala groundwater aquifer between May 22, 2014 and June 27, 2014 (for details of sampling, see text and Fig. S1 in Supporting Information (SI)). Three possible PFAS sources (FFTS-1, FFTS-2, FFTS-3) were considered. Source FFTS-1 consisted of two AFFF training locations (sampling points So1-So4) at a military airport site with historical PFAS-based AFFF usage pre-1985 to 2005. Soil samples at FFTS-1 could only be collected in the vicinity of the hotspot area, since the hotspot area itself has been excavated, with some material removed and the site covered with sandy filling material. Source FFTS-2 consisted of two civil locations (So6-So9) with documented AFFF usage from 1990 until present, while source FFTS-3 comprised one civil location (So10-So12) with documented AFFF usage from 1990 until approximately 1996. At FFTS-1, soil samples were not taken directly from the military training ground because of restricted access, and were instead taken at the perimeter of the facility (see Part S1 in SI). Groundwater samples were collected at four reference locations north of Uppsala (*Björklinge* (G1-G2) (n = 2) and *Storvreta* (G3-G4) (n = 2)), and also at locations slightly north of FFTS-1 (G5-G7) (n = 3), near FFTS-1 (G8-G10) (n = 3), near and below FFTS-2 (G16-G23) (n = 8), near FFTS-3 (G15) (n = 2) and along Uppsala groundwater aquifer (G5-G15, G24-G28) (n = 16). River water samples were collected along the *Fyris river* (W1–W2 and W4–W5) (n = 4) and in its tributary *Sävja river* (W3) (n = 1), where W4 and W5 were located downstream from Uppsala City's major WWTP (*Kungsängsverket*). Outgoing water from *Gränby drinking water treatment plant* to the east of *Uppsala* (D1) (n = 1) was sampled, as was tap water in the west, east, north and south of Uppsala (D2-D4). Sampling dates, coordinates, moisture content [%], organic matter [%], total inorganic carbon [%], total organic carbon [%], total carbon [%], clay [%], silt [%] and sand content [%], pH, temperature [°C], groundwater well elevation [m a.s.l.], depth to water surface [m] pumping level [m] groundwater elevation (m a.s.l.) are shown in Table S1 in SI. For temporal trend analysis of groundwater sampled at G8 and G9 (see section 3.3), samples were collected between 2013 and 2021 (n = 10) (Table S2 in SI).

2.3. PFAS target compounds

In total, 26 PFAS were targeted comprising: four perfluoroalkyl sulfonic acids (PFSA) (PFBS, PFHxS, PFOS, PFDS), 13 perfluoroalkyl carboxylic acids (PFCA) (PFBA, PFPeA, PFHxA, PFHpA, PFOA, PFNA, PFDA, PFUnDA, PFDoDA, PFTriDA, PFTeDA, PFHxDA and PFOcDA), three perfluoroctane sulfonamides (FOSAs) (FOSA, MeFOSA, EtFOSA), two perfluorooctanic sulfonamidoethanols (FOSE) (MeFOSE, EtFOSE), three perfluorooctanic sulfonamide acetates (FOSAA) (FOSAA, MeFOSAA, EtFOSAA) and 6:2 fluorotelomer sulfonate (6:2 FTSA) (for further details, see Table S2 in SI). All samples were fortified with 100 μL of 20 pg μL^{-1} isotopically labelled internal standard mixture (IS) ($^{13}C_8$-FOSA, d_3-MeFOSAA, d_5-EtFOSAA, d_3-MeFOSA, d_5-EtFOSA, d_7-MeFOSE, d_9-EtFOSE, $^{13}C_4$-PFBA, $^{13}C_2$-PFHxA, $^{13}C_4$-PFOA, $^{13}C_5$-PFNA, $^{13}C_2$-PFDA, $^{13}C_2$-PFUnDA, $^{13}C_2$-PFDoDA, $^{18}O_2$-PFHxS, $^{13}C_4$-PFOS), which was used for quantification by the isotope dilution method. In temporal trend

analysis of groundwater, a total of 33 target PFAS were included (Table S3 in SI).

2.4. Sample preparation and PFAS analysis

Soil and sediment samples were analysed using a validated method (Ahrens et al., 2009). In short, all solid and sediment samples were homogenised, sieved to <2 mm and freeze-dried for 48 h, and then 5.0 g dry weight (dw) solids were transferred to 50 mL polypropylene (PP) tubes (Coringer). A two-step solid-liquid extraction was performed, first using 2 mL 100 mM sodium hydroxide in 80:20 methanol:Millipore water, followed by 20 mL of the same solvent spiked with 100 μL IS mixture. In the second step, a further 10 mL of solvent mixture were added. The samples were shaken for 60 min at 200 rpm and centrifuged at 3000 rpm for 15 min, and then decanted and neutralised using 100 μL of 4 M hydrochloric acid. An extract aliquot of 4.15 mL was transferred to a 15 mL PP tube and concentrated to 1 mL using a nitrogen evaporator. For clean-up, 1 mL extract, 25 mg ENVI-carb and 50 μL glacial acetic acid were added to a 1.7 mL PP micro centrifuge tubes (Eppendorf), vortexed for 30 s and centrifuged at 4000 rpm for 10 min. A volume of 0.5 mL was transferred to a 2 mL glass injection vial.

Water samples were analysed according to Ahrens et al. (2009), starting with filtration through pre-heated (550 °C) 0.45 μm glass fibre filters into 1 L PP bottles. Then 0.5 L aliquots were spiked with 100 μL IS mixture and loaded onto a weak anion exchange (WAX) cartridges (500 mg, 60 μm, 6 cc, Oasis, Waters, USA) for solid phase extraction (SPE). The cartridges were pre-conditioned with 4 mL 0.1% ammonium hydroxide in methanol, 4 mL methanol and 4 mL Millipore water. The cartridges were then washed with 4 mL 25 mM ammonium acetate buffer at pH 4, dried and then eluted using 4 mL methanol and 4 mL 0.1% ammonium hydroxide in methanol. The extracts were evaporated with nitrogen gas to 1 mL and transferred to 2 mL glass injection vials.

The analyses were performed by high-performance liquid chromatography (HPLC), using a HP 1100 device (Agilent Technologies, Palo Alto, USA), coupled with tandem mass spectrometry (HPLC-MS/MS) (Agilent G 6410, Agilent Technologies, Palo Alto, USA) with electrospray ionisation (ESI) in negative ionisation mode. For peak separation, a Synergi Hydro RP 80 A column (150 × 2 mm, 4 μm, Phenomenex) was used in combination with a 2 μm Hydro RP Mercury guard column (20 × 2 mm, Synergi, Phenomenex). For data analysis and quantification, MassHunter software version 5 was used.

For temporal trend analysis of groundwater (section 3.3), samples were collected in 250 mL PP bottles from sampling taps directly at the well heads and shipped to ALS Scandinavia in Stockholm, Sweden, for PFAS analysis by liquid chromatography-tandem mass spectrometry (LC-MS/MS) (ISO/IEC 17025). In compliance with US EPA 537 and CSN P CENT/TS, samples were homogenised and filtered before injection if the extract contained particles.

2.5. Quality assurance and quality control

All glassware was washed with distilled water, rinsed with ethanol three times, dish-washed, heated to 400 °C, and rinsed with methanol three times before use. Glass fibre filters were also heated to 400 °C prior to use. PP tubes were rinsed with methanol three times before use. Five duplicate water samples, and one duplicate and three triplicate soil samples, were analysed. For each batch of 10 samples, one duplicate and two laboratory blanks were used for soil/sediment ($n = 3$) and water samples ($n = 10$). The PFAS concentration in laboratory blanks ranged from below method detection limit (MDLs) to 0.64 ng g^{-1} dw (PFBA) for soil/sediment and from below MDL to 3.2 ng L^{-1} (PFDoDA) for water samples (Table S4 in SI). If compounds were detected in blanks, the MDL was calculated from average blank concentration plus three times standard deviation for the individual PFAS, while the lowest calibration point with signal to noise ratio >3 was used for PFAS not detected in blank samples. The MDL for soil/sediment samples ranged from 0.01 ng g^{-1} dw to 1.2 ng g^{-1} dw (PFBA), and the MDL for water samples ranged from 0.1 ng L^{-1} to 14 ng L^{-1} (PFDoDA) (Table S4 in SI). Relative recovery, based on the average ratio of peak area of IS in samples compared with the calibration curves, ranged from 88 ± 11% ($^{13}C_5$ PFNA) to 130 ± 13% ($^{13}C_4$-PFOA) for soil/sediment and from 43 ± 19% (d_9-EtFOSE) to 97 ± 24% (d_3-MeFOSAA) for water samples (Table S5 in SI). The difference between duplicate samples ranged from <1% (6:2 FTSA in water) to 52% (PFDoDA in soil). For temporal trend analysis of groundwater, one blank sample, one spiked sample and one duplicate sample were analysed every 20 samples.

2.6. Statistical analysis

Investigation of relationships between samples was performed by principal component analysis (PCA) using Canaco software and normalised data. This approach was used for enabling fingerprinting analysis and source tracing (Möller et al., 2010; Sörengård et al., 2020a). The model input was the compositional profiles of individual PFAS in each sample [fraction 0–1], obtained by dividing concentration of individual PFAS by total PFAS concentration. For statistical analysis, concentrations < MDL were excluded and, because of low concentrations, some samples (G1-G6, G28) were removed from the analysis (Table S6 in SI). Mean centring and autoscaling to unit variance were applied.

3. Results and discussion

3.1. Spatial distribution of PFAS

3.1.1. Soil and sediment

At the three FFTS investigated, a total of 25 out of 26 target PFAS were detected in at least one soil or sediment sample (So1-So12, Se1–Se2) (Fig. 1, Table S6 in SI). At FFTS-1 (samples So1-So4, taken at the perimeter of the military base), PFOS was the dominant compound, with an average concentration of 75 ng g^{-1} dw (70% of ∑PFAS) in So1-So2 and 7 ng g^{-1} dw (67% of ∑PFAS) in So3-So4, followed by FOSA (13%) and PFPeA (6%). These relatively low concentrations are likely the result of the earlier excavation and removal of highly contaminated material at the site. High PFAS concentrations were also found at the nearby military area outside the FFTS area (So5), with a ∑PFAS concentration of 140 ng g^{-1} dw dominated by PFOS (91%), indicating that PFAS concentrations are elevated not only at the FFTS itself, but also nearby. This is possibly due to unrecorded firefighting action, aerosol transport of PFAS, storm water run-off, cleaning of fire training equipment, and even leaky wastewater or stormwater pipelines.

Unlike FFTS-1, FFTS-2 samples (So6-So9) were taken directly at the hotspot where PFAS-containing AFFF was used in the past, according to staff at the site. Thus, PFAS soil concentrations were considerably higher than at FFTS-1, with an average ∑PFAS concentration of 560 ng g^{-1} dw in So8 and 180 ng g^{-1} dw in So9, both dominated by PFOS (81% of ∑PFAS). However, the PFAS concentrations at FFTS-1 was most likely underestimated, since it was not possible to collect samples from the top soil layers in the actual hotspot area. In the FFTS-2 drainage pond sediment, the ∑PFAS concentration was 470 ng g^{-1} dw (Se1) and 350 ng g^{-1} dw (Se2) (PFOS ~84% of ∑PFAS).

At FFTS-3 (samples So10-So12), ∑PFAS concentrations were low, <2.8 ng g^{-1} dw, which is similar to soil background concentrations in Sweden (Sörengård et al., 2022).

In general, PFOS was the dominant compound in the soil and sediment samples analysed in this study, which is in agreement with findings in most other studies on AFFF-affected soils (reviewed in Brusseau et al., 2020). However, the maximum PFOS level recorded, 490 ng g^{-1} dw at So9, was at the lower end of the range reported for other AFFF-affected firefighting training areas, e.g. median concentration 8700 ng g^{-1} dw and maximum concentration 373 000 ng g^{-1} dw at an AFFF-impacted site on a U.S. Air Force base (Brusseau et al., 2020). High concentrations of PFOS can persist in the top 1–3 m soil layer long after release of

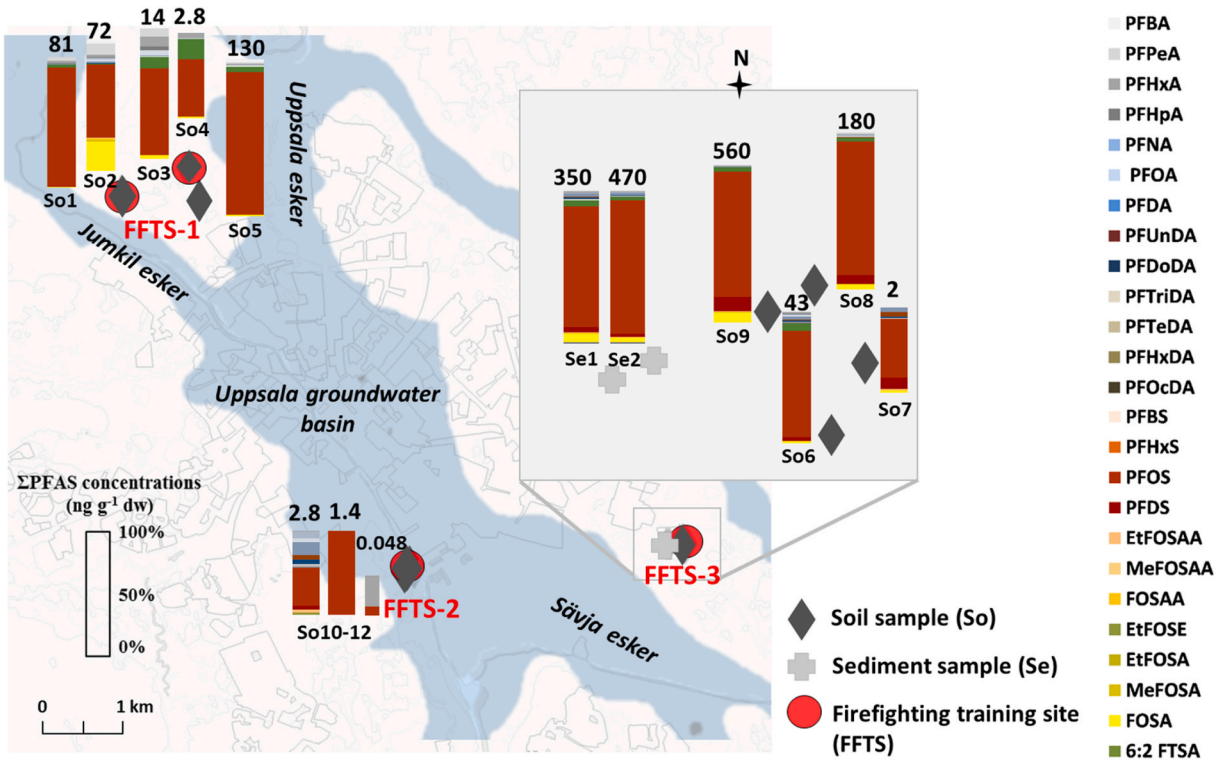

Fig. 1. Composition profiles (fraction of $\sum_{26}$PFAS) in soil (So) and sediment (Se) and Σ_{26}PFAS concentrations in ng g^{-1} dw at the different sampling sites.

AFFF, as shown in soil column field studies (Høisæter et al., 2019; Brusseau et al., 2020), experiments (Høisæter et al., 2019) and mathematical modelling (Guo et al., 2020). Topsoil sampling can be problematic because of spatial heterogeneity within a source zone (Filipovic et al., 2015a).

3.1.2. Groundwater

In total, 18 out of 26 target PFAS were detected at least once in groundwater samples (G1-G28), with PFHxS (68% of samples), PFPeA (64%), PFOS (57%), PFBS (50%) and PFHxA (50%) most frequently detected (Fig. 2, Table S6 in SI). Groundwater concentrations and composition differed with proximity to the different FFTS. Just downgradient from FFTS-1, groundwater samples G8 and G9 from monitoring wells extending 33 and 16 m below ground surface, respectively, had high ΣPFAS concentrations, up to 1000 ng L^{-1} at G9 and 280 ng L^{-1} at G8. The main substances detected were PFHxS (58–62% of ∑PFAS), PFOS (15–16%), PFHxA (8–12%) and PFBS (8–9%). Up-gradient of FFTS-1, samples from *Jumskil esker* (G1-G2 and G3-G4, 17 and 10 km away, respectively) and from the main Uppsala groundwater aquifer (G5-G7, G10; 1.5–3 km away) showed low PFAS concentrations (<MDL to 3 ng L^{-1}). This indicates that the PFAS contamination originated from FFTS-1, probably via *Jumskil esker*. Potential pollutant transport pathways from FFTS-1 to groundwater could be through moraine soil layers and along shallow fractures in bedrock. Previous laboratory and computational studies have shown that the mobility of PFAS depends on their perfluorocarbon chain length, functional group and water and soil characteristics (Ochoa-Herrera and Sierra-Alvarez, 2008; Zhang et al., 2014; Campos Pereira et al., 2018; Kibbey et al., 2021). In-field observations of PFAS mobility are largely lacking (Tokranov et al., 2021).

South of FFTS-1 the PFAS concentration gradually decreased, with concentrations of 220 ng L^{-1} to 64 ng L^{-1} (G12-G15) and, further southward, 57 ng L^{-1} to 1.3 ng L^{-1} (G24-G27) (Fig. 2). This decrease, by a factor of around 2–12, is in line with the dilution factor between the contaminated aquifer (*Jumkil esker*), with flow rate 5–25 L/s (Vatteninformationssystem Sverige, 2022), and *Uppsala esker* with flow rate 125 L/s and mixing efficiency 50%. The average PFAS composition profile at sampling points G12-G14 was similar to that at G8 and G9, with PFHxS (51% of ∑PFAS), PFBS (19%), PFOS (13%) and PFHxA (6.7%) (for detailed discussion, see section 3.2). Farther south of the drinking water wellfields (G24-G26) the contribution changed slightly, with an increase in PFHxS (54% of ∑PFAS), a decrease in PFOS (3.1%), and presence of PFBS (11%), PFHxA (8.1%) and PFOA (6.0%). The percentage of PFHxS of the sum concentration of PFHxS + PFOS as a function of distance from G9 near FFTS-1 significantly increased ($p < 0.001$), while at the same time the percentage of PFOS significantly decreased ($p < 0.001$) (Fig. S2 in SI). The increase of the PFHxS over distance down-gradient of the source zone can be explained by the lower soil sorption strength of PFHxS compared with PFOS (Campos Pereira et al., 2018). Farther south of the urban city centre (G24-G28) and of FFTS-3, there was no apparent influence of another PFAS source, with the ∑PFAS concentration gradually decreasing to 1 ng L^{-1} at G27 and <MDL at G28. This decrease is most likely explained by dilution along the aquifer originating from infiltration from surrounding vadose zones, although G27 could also be impacted by concentrations in Lake Ekoln, because of its close proximity (section 3.1.3).

FFTS-2 showed also high PFAS contamination of the soil, dominated by PFOS (Fig. 1). However, in contrast to FFTS-1, the PFAS composition profile in groundwater near the hotspot area at FFTS-2 (G16-G20, G22-G23) generally reflected the soil PFAS composition profile, which was dominated by PFOS. The highest ∑PFAS concentrations were found at G21 (8000 ng L^{-1}) and G17 (2100 ng L^{-1}), with considerably higher 6:2 FTSA levels at G21 (5400 ng L^{-1}, 61% of ΣPFAS). In contrast, 6:2 FTSA was not found in Uppsala groundwater aquifer. The detection of 6:2 FTSA reflects a usage shift from PFOS-containing AFFF to PFAS precursor-containing AFFF, which are later degraded into perfluorinated PFAS species (Ahrens, 2011; Land et al., 2018). AFFF-affected soils are known to contain a significant amount of PFAS precursors, encompassing over 100 species with varying properties (Houtz et al., 2013; Martin et al., 2019; Nickerson et al., 2021), but analytical challenges remain in assessing these.

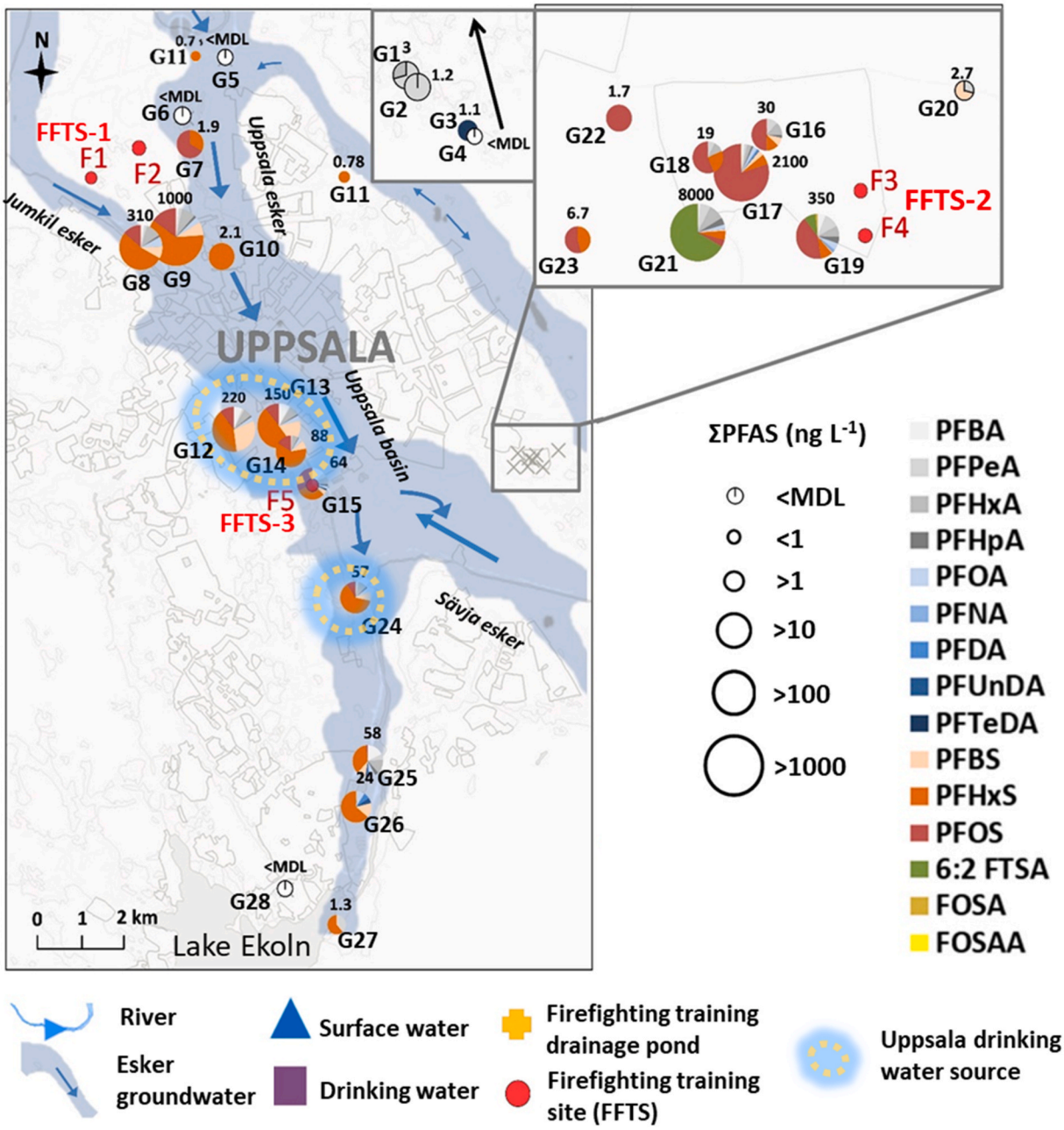

Fig. 2. Composition profiles (pie charts) and Σ_{26}PFAS concentrations [ng L^{-1}] of detected PFAS in samples of groundwater (G1-G28). Firefighting training sites are indicated as FFTS-1 (F1, F2), FFTS-2 (F3, F4) and FFTS-3 (F5). Average values are given for sampling points G1, G6, G8 G10, G11, G12 and G20.

3.1.3. *Surface water*

In the FFTS-2 drainage pond surface water (W6), discharged into Sävja river (W3), 18 out of 26 target PFAS were detected, with a ΣPFAS concentration of 3000 ng L^{-1}. The contribution of 6:2 FTSA was higher than in any other surface water sample (25% of ∑PFAS), indicating that use of PFAS precursor-containing AFFF and soil contamination is reflected in run-off water. The high concentration of PFAS confirms that FFTS can also affect nearby surface water (Houde et al., 2008; Koch et al., 2021).

In contrast to the soil and groundwater samples, only four (PFPeA, PFHxA, PFHxS, PFOS) of the 26 target PFAS were found in surface river water (W1–W5) (Fig. 3, Table S6 in SI). The ΣPFAS concentration ranged from <MDL to 15 ng L^{-1} and was dominated by PFOS and PFHxS (80% of ΣPFAS). Minor, but still increasing, concentration changes were observed in the gradient on passing through urban areas of Uppsala City, most likely due to point sources such as the municipal wastewater treatment plant and FFTS-3. The ΣPFAS concentration in the Fyris river upstream of the urban area was <MDL (W1), followed by 8 ng L^{-1} at W2. In Sävja river water (W3) it was 15 ng L^{-1} and in samples from the southern part of the Fyris River (W4–W5) it was 13 and 11 ng L^{-1}, respectively.

Outflow from the Fyris river estuary into Lake Ekoln, which is part of Lake Mälaren, Sweden's largest source of drinking water, was estimated based on the southernmost river sampling point (W5). The ∑PFAS concentration was multiplied by modelled river flow rate [m^3 s^{-1}] based on data acquired from the Swedish Meteorological and Hydrological Institute (SMHI, 2014) (Table S7 in SI). The highest estimated ΣPFAS flux was on average 60 g day^{-1} (14 kg $year^{-1}$), with 19 g day^{-1} (6.8 kg $year^{-1}$) of PFHxS, followed by 18 g day^{-1} (6.5 kg $year^{-1}$) of PFOS (Table S7 in SI). Thus, the inflow of PFAS into Lake Mälaren is

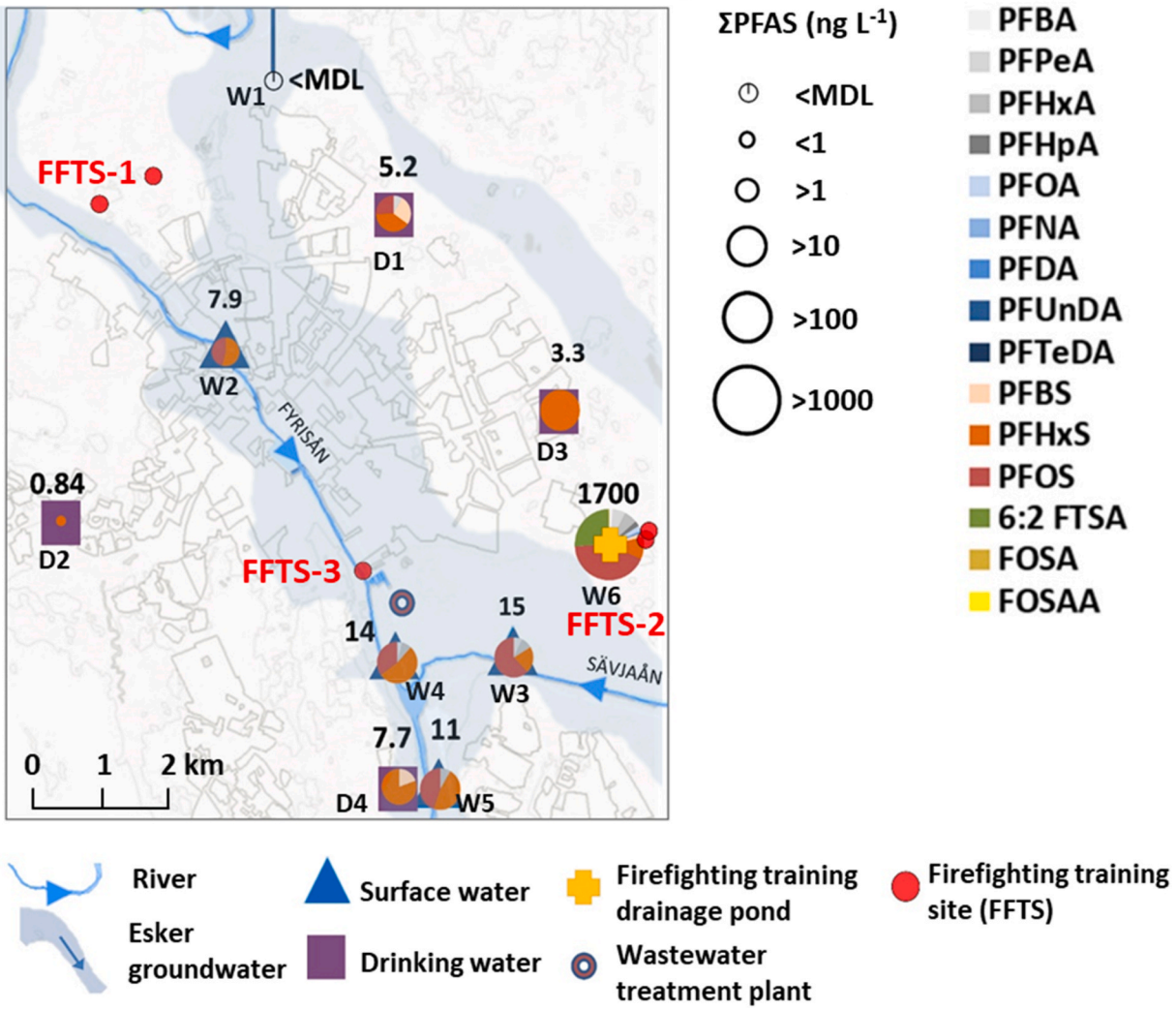

Fig. 3. Composition profiles (pie charts) and Σ_{26}PFAS concentrations [ng L^{-1}] of detected PFAS in samples of surface water (W1–W5), an FFTS drainage pond (W6) and tap water (D1-D4). Firefighting training sites are indicated as FFTS-1, FFTS-2 and FFTS-3. Average values are given for sampling point W6.

considerable. Detection of PFAS at a drinking water treatment plant using raw water from Lake Mälaren, which supplies Stockholm with drinking water, has recently been reported (Tröger et al., 2018; Ullberg et al., 2021). Although $\sum_{11}$PFAS concentrations at Stockholm's drinking raw water were relatively low (7.4 ng L^{-1}), removal efficiencies of PFAS at Stockholm's drinking water treatment plant were low (<10%) and higher $\sum_{11}$PFAS concentrations were found at Lake Ekoln near Uppsala (15 ng L^{-1}), which will eventually be transported to Stockholm's drinking raw water area (Tröger et al., 2018).

3.1.4. Drinking water

In total, four out of 26 target PFAS were detected in the drinking water samples (D1-D4) and the ΣPFAS concentration ranged from 1.0 ng L^{-1} (D2) to 8.0 ng L^{-1} (D4) (Fig. 3, Table S6 in SI). Uppsala drinking water is known to have elevated PFOS, PFHxS and PFBS concentrations, resulting in exposure in humans (e.g. Gyllenhammar et al., 2015). Activated carbon filters have been installed to remove PFAS (Belkouteb et al., 2020), resulting in PFAS levels in outgoing water (samples D1-D4) that were below Swedish and European Union drinking water guideline values of 90 ng L^{-1} for $\sum_{11}$PFAS and 100 ng L^{-1} for $\sum_{20}$PFAS, respectively (Gobelius et al., 2018; European Commission, 2020). PFHxS was the most frequently detected PFAS in drinking water, reflecting the relative higher abundance of this compound in the deep esker groundwater drinking source. PFBS has shown to be more mobile than PFHxS and PFOS and has a lower removal efficiency using activated carbon filters (McCleaf et al., 2017). Although there is considerable presence of PFAS in the drinking water aquifer, time trend analysis of human blood serum samples has shown that previously elevated PFAS levels in affected cohorts have decreased considerably since 2012 (Gyllenhammar et al., 2015; Stubleski et al., 2016; Miaz et al., 2020; Glynn et al., 2020). This is strongly related to more efficient PFAS removal in the drinking water treatment plant (McCleaf et al., 2017; Belkouteb et al., 2020), which demonstrates that mitigation actions can have successful outcomes and that efficient PFAS water treatment techniques should continue to be developed.

3.2. Source tracing

The PFAS composition profile in groundwater samples (i.e. PFAS fingerprint) (Möller et al., 2010; Sörengård et al., 2020a) was compared using PCA analysis, to trace the source of PFAS contamination in groundwater. The PCA results showed that PC1 and PC2 explained 40% and 24% of the variation in the data (Fig. 4), respectively. The loading plot showed that for PC1, PFOS and PFDS were the compounds with the highest impact, while for PC2 PFOS, PFHxS and PFHxA had the highest impact. Fig. 4 shows the PFAS compositional profile in groundwater at FFTS-1 (G8-G9 (green)) clustering with the groundwater samples along the southward aquifer flow (G10-G14 and G24-G27). The FFTS-2

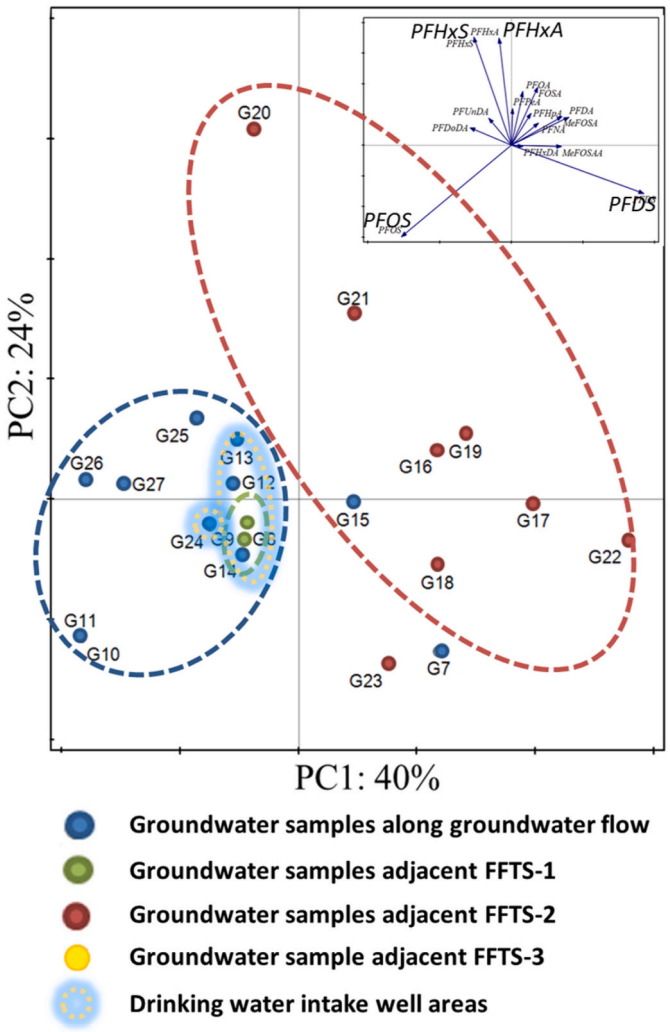

Fig. 4. Principal component analysis (PCA) score plot (main diagram) and loading plot (upper right corner) of composition profiles (fraction of individual $\sum_{26}$PFAS) in groundwater from the different sites. Green dots represent groundwater samples near firefighting training site FFTS-1 (G8-G9), red dots represent FFTS-2 (G16-G23) and blue dots represent groundwater samples along the direction of flow (G7, G10-G15, G24-G27). The monitoring wells at points G12-G14 (marked in transparent blue and yellow dotted line) are in close proximity to the main intake well for a major Uppsala drinking water treatment plant. G11 and G10 have the same PFAS composition profile and thus lie on top of each other. Principal components PC1 and PC2 together explained 64% of the variance. (For interpretation of the references to colour in this figure legend, the reader is referred to the Web version of this article.)

(G16-G23) scores clustered separately, indicating a different source than deep aquifer contamination. The FFTS-3 scores (G15) were located between the two clusters, which might indicate an impact on the aquifer. However, this is unlikely as elevated groundwater concentrations were not observed downstream of FFTS-3 (see section 3.1.2).

Ultimately, based on the PFAS fingerprints in PCA and elevated PFAS concentrations with close proximity between FFTS and aquifer, the results indicate that FFTS-1 is the more probable original source of PFAS contamination in Uppsala groundwater aquifer. This means that the PFAS plume has migrated >10 km (from G9 to G26), which can be explained by high hydraulic conductivity and low PFAS sorption strength in the coarse glaciofluvial esker (Campos Pereira et al., 2018; Sorengard et al., 2019). Few previous studies have reported such long-distance transport of PFAS in an aquifer, although contamination of an aquifer 2 km downstream from two FFTS using PFAS-containing AFFF has been reported (Dauchy et al., 2019). Uppsala groundwater aquifer is located in an urban area, so other alternative sources cannot be ruled out, such as AFFF from vehicle or structural fires, industrial discharges, wastewater treatment plants and abandoned landfills. However, no alternative source is known to have utilised sufficiently large AFFF quantities to explain the PFAS concentrations in groundwater in the aquifer.

Another industrial site located 1–2 km west of FFTS-2, and in close proximity to Uppsala groundwater aquifer, is known to have released AFFF, and a comprehensive external investigation was conducted in 2019 (AECOM Report, 2020). The presence of PFAS was identified in all groundwater monitoring wells (n = 63), which included both perched and deeper groundwater, and in the deeper moraine groundwater (n = 26). Some samples showed Σ_{11}PFAS levels exceeding 10 000 ng L^{-1}. In most (67%) of the monitoring wells, the compositional profile showed large proportions of PFOS and 6:2 FTSA (otherwise a homogeneous mix), which differed from the PFAS compositional profile observed in Uppsala groundwater aquifer in this study, where PFHxS was the most prominent PFAS. In addition, 6:2 FTSA was not found (all levels < MDL) in Uppsala groundwater aquifer in the present study, indicating that this particular industrial site was most likely not the main source of the PFAS pollution observed in Uppsala City's wellfield or degradation of 6:2 FTSA during transport (Merino et al., 2016). The PFAS composition can still change down-gradient of the source zone, e.g. because of the lower soil sorption strength of PFHxS compared with PFOS (Campos Pereira et al., 2018) the fraction of PFHxS can increase over distance. It has been shown that 6:2 FTSA has similar sorption strength as PFHxS (Campos Pereira et al., 2018; Sorengard et al., 2019). However, no increasing fraction of 6:2 FTSA was observed in the samples from Uppsala groundwater aquifer, a further indication that the industrial site in question did not cause the main PFAS contamination of the aquifer. Ultimately, this example shows the complex nature of source tracing in urban areas, with additional sources continually being identified over time.

3.3. Temporal trends

Monitoring well G9 at FFTS-1 had the highest levels of PFAS recorded in this study (Fig. 2A, year 2014), during long-term monitoring of Σ_{33}PFAS concentrations at FFTS-1 since 2013 (Fig. 5B). Regression analysis of the eight-year time trend showed a significant decrease in Σ_{33}PFAS concentration 2013–2021 (r^2 = 0.68, p < 0.01), of 0.29 log units per year. Comparison of Σ_{33}PFAS concentrations in groundwater in June 2021 with those at the first sampling in October 2013 showed that the concentration had decreased by 99.7% (from 2300 ng L^{-1} to 71 ng L^{-1}). On the other hand, adjacent monitoring well G8, located closer to *Jumskil esker*, showed no significant decreasing linear regression time trend (p > 0.05) (Fig. 5A), which could be explained by its location closer to a continuous point source at FFTS-1. Historically, PFAS-based AFFF has been used at FFTS-1 between pre-1985 and 2005, and thus PFAS-based AFFF has not been used after the first sampling in October 2013. The relative stable ∑PFAS concentration at G8 indicates that PFAS has been leached out from FFTS-1 even after discontinuation of the use of PFAS-based AFFF and impacted G8 at least until 2021. At the end of the monitoring period (2021), G8 had considerably higher Σ_{33}PFAS levels (860 ng L^{-1}) than G9 (70 ng L^{-1}). Sampling point G9 is located at the confluence of *Jumskil esker* and *Uppsala esker* and is thus impacted by two different source waters with seasonally varying magnitude. *Uppsala esker* has a higher flow rate and is supplemented by infiltrated water from Uppsala City's MAR system.

In the G8 and G9 monitoring wells, the Σ_{33}PFAS concentration showed high fluctuations, e.g. it increased by a factor of 3, from 88 ng L^{-1} to 380 ng L^{-1}, in monitoring well G9 between June 2020 and September 2020. A previous time trend study in the monitoring well showed 2-fold variation over three years (2012–2014) (Gyllenhammar et al., 2015). This type of large variations in PFAS groundwater

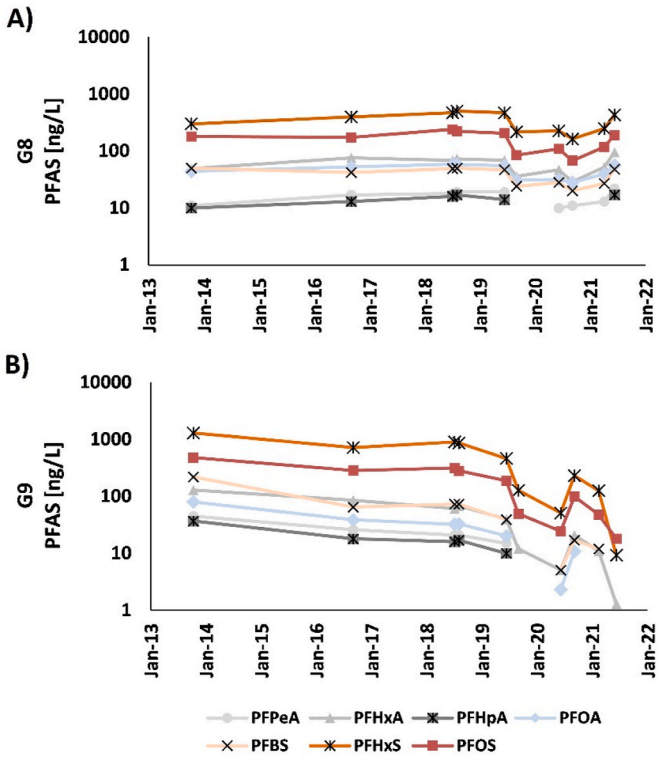

Fig. 5. PFAS concentrations 2013–2021 [ng L^{-1}] in monitoring wells G8 (A) and G9 (B), located close to FFTS-1.

concentration over time may be influenced by transport changes in the aquifer due to variations in seasonal groundwater flows, dilution, chemical changes such as pH (Du et al., 2014), Uppsala City's MAR system, and variations in the rate of PFAS leaching from contaminated soil due to precipitation events and snowmelt. The PFAS decrease was not significantly correlated with water level in the well ($p > 0.05$) (Fig. S3 in SI), but presence of dilution effects is still supported by the strong correlation between individual PFAS over time for PFHxA, PFOA, PFBS, PFHxS and PFOS ($r^2 = 0.81–0.97$, mean = 0.89) (Table S8 in SI), since the PFAS species would be affected differently by changes in source depletion and chemical fluctuations (Du et al., 2014). The low variation in compositional profile found in time trend monitoring means that the fingerprinting analysis (section 3.2, Fig. 4) can probably be extrapolated over time, but further data on PFAS concentrations over time are needed for validation.

4. Conclusions

Comprehensive analysis of PFAS concentrations in the Uppsala drinking water aquifer revealed that contamination was greatest in groundwater and was most likely caused by FFTS-1. This firefighting training site has used PFAS-containing AFFF in the past, and based on topography, drains to aquifer used for drinking water production. Quantification of PFAS levels showed that the esker-based drinking water aquifer had groundwater ΣPFAS concentrations of up to 1000 ng L^{-1}, dominated by PFHxS and PFOS. The complexity of PFAS transport from source to groundwater was illustrated by highly contaminated aquifer monitoring wells at FFTS-1. The ΣPFAS concentration was one order of magnitude lower down-gradient, probably because of dilution with water from the northern Uppsala groundwater aquifer. PCA analysis of the PFAS compositional profile showed a strong association of PFAS concentrations at FFTS-1 and the groundwater drinking water source area, and a weak association of PFAS concentrations at FFTS-2. Eight-year time trend analysis (2013–2021) of the most contaminated monitoring well near FFTS-1 showed a transitory decrease of up to 99.6% by 2021, resulting in a ΣPFAS concentration of 7.1 ng L^{-1}, which is below the drinking water guideline value of 90 ng L^{-1}. The decrease in concentration can be attributed to a net flux reduction from the source and dilution effects, considering the stable PFAS compositional profile.

Surface waters were contaminated with PFAS and may have been affected by FFTS surface runoff, but also by WWTP effluents and diffuse sources. The main river was estimated to transport approximately 14 kg $year^{-1}$ downstream to Sweden's largest drinking water source area, Lake Mälaren. The ∑PFAS concentrations in consumer tap water were found to be far lower than in the drinking water aquifer, with a maximum of 7.7 ng L^{-1}, which can be attributed to installation of activated carbon filtration in the drinking water treatment plant, which has decreased PFAS levels in human serum over time according to previous studies. The aquifer is currently mostly contaminated with PFHxS, while the soil at the hot-spot sites FFTS-1 and FFTS-2 is predominantly contaminated by the slowly leaching PFOS. Thus, strategies for sustainable management of the contaminated aquifer should be based on continued monitoring of PFAS in both the aquifer and drinking water. This can verify the PFAS concentration time trend, support assessment of human health risks and determine the effects of previous (pre-2012) human exposure to unknown, but probably higher, levels of PFAS in the drinking water.

Author statement

Mattias Sörengård: Writing - Original draft preparation, Data curation, Visualization, Validation. **Sofia Bergström**: Methodology, Data curation, Visualization, Validation, Writing – original draft preparation. **Philip McCleaf**: Conceptualization, Visualization, Writing – review & editing. **Karin Wiberg**: Supervision, Writing – review & editing. **Lutz Ahrens**: Conceptualization, Supervision, Validation, Writing – review & editing.

Declaration of competing interest

The authors declare that they have no known competing financial interests or personal relationships that could have appeared to influence the work reported in this paper.

Data availability

Data will be made available on request.

Appendix A. Supplementary data

Supplementary data to this article can be found online at https://doi.org/10.1016/j.envpol.2022.119981.

References

AECOM Report, 2020. PFAS Conceptual Site Model Report. Project Number: 60599350. October 19.

Ahrens, L., 2011. Polyfluoroalkyl compounds in the aquatic environment: a review of their occurrence and fate. J. Environ. Monit. 13, 20–31. https://doi.org/10.1039/C0EM00373E.

Ahrens, L., Barber, J.L., Xie, Z., Ebinghaus, R., 2009. Longitudinal and latitudinal distribution of perfluoroalkyl compounds in the surface water of the atlantic ocean. Environ. Sci. Technol. 43, 3122–3127. https://doi.org/10.1021/es803507p.

Ahrens, L., Norström, K., Viktor, T., Cousins, A.P., Josefsson, S., 2015. Stockholm Arlanda Airport as a source of per- and polyfluoroalkyl substances to water, sediment and fish. Chemosphere 129, 33–38. https://doi.org/10.1016/j.chemosphere.2014.03.136.

Baduel, C., Paxman, C.J., Mueller, J.F., 2015. Perfluoroalkyl substances in a firefighting training ground (FTG), distribution and potential future release. J. Hazard Mater. 296, 46–53. https://doi.org/10.1016/j.jhazmat.2015.03.007.

Belkouteb, N., Franke, V., McCleaf, P., Köhler, S., Ahrens, L., 2020. Removal of per- and polyfluoroalkyl substances (PFASs) in a full-scale drinking water treatment plant: long-term performance of granular activated carbon (GAC) and influence of flow-rate. Water Res. 182, 115913 https://doi.org/10.1016/j.watres.2020.115913.

Benskin, J.P., Li, B., Ikonomou, M.G., Grace, J.R., Li, L.Y., 2012. Per- and polyfluoroalkyl substances in landfill leachate: patterns, time trends, and sources. Environ. Sci. Technol. 46, 11532–11540. https://doi.org/10.1021/es302471n.

Brusseau, M.L., Anderson, R.H., Guo, B., 2020. PFAS concentrations in soils: background levels versus contaminated sites. Sci. Total Environ. 740, 140017 https://doi.org/10.1016/j.scitotenv.2020.140017.

Buck, R.C., Franklin, J., Berger, U., Conder, J.M., Cousins, I.T., Voogt, P.D., Jensen, A.A., Kannan, K., Mabury, S.A., van, L., 2011. Perfluoroalkyl and polyfluoroalkyl substances in the environment: terminology, classification, and origins. Integrated Environ. Assess. Manag. 7, 513–541. https://doi.org/10.1002/ieam.258.

Busch, J., Ahrens, L., Sturm, R., Ebinghaus, R., 2010. Polyfluoroalkyl compounds in landfill leachates. Environ. Pollut. 158, 1467–1471. https://doi.org/10.1016/j.envpol.2009.12.031.

Campos Pereira, H., Ullberg, M., Kleja, D.B., Gustafsson, J.P., Ahrens, L., 2018. Sorption of perfluoroalkyl substances (PFASs) to an organic soil horizon – effect of cation composition and pH. Chemosphere 207, 183–191. https://doi.org/10.1016/j.chemosphere.2018.05.012.

Chelcea, I.C., Ahrens, L., Örn, S., Mucs, D., Andersson, P.L., 2020. Investigating the OECD database of per- and polyfluoroalkyl substances-chemical variation and applicability of current fate models. Environ. Chem. 17, 498–508. https://doi.org/10.1071/EN19296.

Dauchy, X., Boiteux, V., Colin, A., Hémard, J., Bach, C., Rosin, C., Munoz, J.-F., 2019. Deep seepage of per- and polyfluoroalkyl substances through the soil of a firefighter training site and subsequent groundwater contamination. Chemosphere 214, 729–737. https://doi.org/10.1016/j.chemosphere.2018.10.003.

DeWitt, J.C. (Ed.), 2015. Toxicological Effects of Perfluoroalkyl and Polyfluoroalkyl Substances, Molecular and Integrative Toxicology. Humana Press, Cham Heidelberg.

Du, Z., Deng, S., Bei, Y., Huang, Q., Wang, B., Huang, J., Yu, G., 2014. Adsorption behavior and mechanism of perfluorinated compounds on various adsorbents—a review. J. Hazard Mater. 274, 443–454. https://doi.org/10.1016/j.jhazmat.2014.04.038.

European Commission, 2020. COMMUNICATION FROM THE COMMISSION TO THE EUROPEAN PARLIAMENT. THE COUNCIL, THE EUROPEAN ECONOMIC AND SOCIAL COMMITTEE AND THE COMMITTEE OF THE REGIONS, Brussels.

European Food Safety Authority (EFSA), 2012. Perfluoroalkylated substances in food: occurrence and dietary exposure. EFSA J. 10 https://doi.org/10.2903/j.efsa.2012.2743.

Filipovic, M., Woldegiorgis, A., Norström, K., Bibi, M., Lindberg, M., Österås, A.-H., 2015a. Historical usage of aqueous film forming foam: a case study of the widespread distribution of perfluoroalkyl acids from a military airport to groundwater, lakes, soils and fish. Chemosphere 129, 39–45. https://doi.org/10.1016/j.chemosphere.2014.09.005.

Filipovic, M., Woldegiorgis, A., Norström, K., Bibi, M., Lindberg, M., Österås, A.-H., 2015b. Historical usage of aqueous film forming foam: a case study of the widespread distribution of perfluoroalkyl acids from a military airport to groundwater, lakes, soils and fish. Chemosphere 129, 39–45. https://doi.org/10.1016/j.chemosphere.2014.09.005.

Franke, V., Ullberg, M., McCleaf, P., Wålinder, M., Köhler, S.J., Ahrens, L., 2021. The price of really clean water: Combining nanofiltration with granular activated carbon and anion exchange resins for the removal of per- and polyfluoralkyl substances (PFASs) in drinking water production. ACS ES&T Water 1, 782–795. https://doi.org/10.1021/acsestwater.0c00141.

Gellrich, V., Brunn, H., Stahl, T., 2013. Perfluoroalkyl and polyfluoroalkyl substances (PFASs) in mineral water and tap water. J. Environ. Sci. Health Part Toxic Hazard. Subst. Environ. Eng. 48, 129–135. https://doi.org/10.1080/10934529.2013.719431.

Glynn, A., Kotova, N., Dahlgren, E., Lindh, C., Jakobsson, K., Gyllenhammar, I., Lignell, S., Nälsén, C., 2020. Determinants of serum concentrations of perfluoroalkyl acids (PFAAs) in school children and the contribution of low-level PFAA-contaminated drinking water. Environ. Sci. Process. Impacts 22, 930–944. https://doi.org/10.1039/c9em00497a.

Gobelius, L., Hedlund, J., Dürig, W., Tröger, R., Lilja, K., Wiberg, K., Ahrens, L., 2018. Per- and polyfluoroalkyl substances in Swedish groundwater and surface water: implications for environmental quality standards and drinking water guidelines. Environ. Sci. Technol. 52, 4340–4349. https://doi.org/10.1021/acs.est.7b05718.

Guelfo, J.L., Higgins, C.P., 2013. Subsurface transport potential of perfluoroalkyl acids at aqueous film-forming foam (AFFF)-Impacted sites. Environ. Sci. Technol. 47, 4164–4171. https://doi.org/10.1021/es3048043.

Guo, B., Zeng, J., Brusseau, M.L., 2020. A mathematical model for the release, transport, and retention of per- and polyfluoroalkyl substances (PFAS) in the vadose zone. Water Resour. Res. 56 https://doi.org/10.1029/2019WR026667.

Gyllenhammar, I., Berger, U., Sundström, M., McCleaf, P., Eurén, K., Eriksson, S., Ahlgren, S., Lignell, S., Aune, M., Kotova, N., Glynn, A., 2015. Influence of contaminated drinking water on perfluoroalkyl acid levels in human serum - a case study from Uppsala, Sweden. Environ. Res. 140, 673–683. https://doi.org/10.1016/j.envres.2015.05.019.

Hale, S.E., Arp, H.P.H., Slinde, G.A., Wade, E.J., Bjørseth, K., Breedveld, G.D., Straith, B.F., Moe, K.G., Jartun, M., Høisæter, Å., 2017. Sorbent amendment as a remediation strategy to reduce PFAS mobility and leaching in a contaminated sandy soil from a Norwegian firefighting training facility. Chemosphere 171, 9–18. https://doi.org/10.1016/j.chemosphere.2016.12.057.

Herzke, D., Olsson, E., Posner, S., 2012. Perfluoroalkyl and polyfluoroalkyl substances (PFASs) in consumer products in Norway - a pilot study. Chemosphere 88, 980–987. https://doi.org/10.1016/j.chemosphere.2012.03.035.

Høisæter, Å., Pfaff, A., Breedveld, G.D., 2019. Leaching and transport of PFAS from aqueous film-forming foam (AFFF) in the unsaturated soil at a firefighting training facility under cold climatic conditions. J. Contam. Hydrol. 222, 112–122. https://doi.org/10.1016/j.jconhyd.2019.02.010.

Houde, M., Czub, G., Small, J.M., Backus, S., Wang, X., Alaee, M., Muir, D.C.G., 2008. Fractionation and bioaccumulation of perfluorooctane sulfonate (PFOS) isomers in a lake ontario food web. Environ. Sci. Technol. 42, 9397–9403. https://doi.org/10.1021/es800906r.

Houtz, E.F., Higgins, C.P., Field, J.A., Sedlak, D.L., 2013. Persistence of perfluoroalkyl acid precursors in AFFF-impacted groundwater and soil. Environ. Sci. Technol. 47, 8187–8195. https://doi.org/10.1021/es4018877.

Houtz, E.F., Sutton, R., Park, J.-S., Sedlak, M., 2016. Poly- and perfluoroalkyl substances in wastewater: significance of unknown precursors, manufacturing shifts, and likely AFFF impacts. Water Res. 95, 142–149. https://doi.org/10.1016/j.watres.2016.02.055.

Kibbey, T.C.G., Jabrzemski, R., O'Carroll, D.M., 2021. Predicting the relationship between PFAS component signatures in water and non-water phases through mathematical transformation: application to machine learning classification. Chemosphere 282, 131097. https://doi.org/10.1016/j.chemosphere.2021.131097.

Koch, A., Wang, T., Jonsson, M., Yeung, L.W.Y., Kärrman, A., Ahrens, L., Ekblad, A., 2021. Quantification of biodriven transfer of per- and polyfluoroalkyl substances from the aquatic to the terrestrial environment via emergent insects. Environ. Sci. Technol. 55, 7900–7909. https://doi.org/10.1021/acs.est.0c07129.

Land, M., de Wit, C.A., Bignert, A., Cousins, I.T., Herzke, D., Johansson, J.H., Martin, J.W., 2018. What is the effect of phasing out long-chain per- and polyfluoroalkyl substances on the concentrations of perfluoroalkyl acids and their precursors in the environment? A systematic review. Environ. Evid. 7, 4. https://doi.org/10.1186/s13750-017-0114-y.

Lemal, D.M., 2004. Perspective on fluorocarbon chemistry. J. Org. Chem. 69, 1–11. https://doi.org/10.1021/jo0302556.

Li, Y., Fletcher, T., Mucs, D., Scott, K., Lindh, C.H., Tallving, P., Jakobsson, K., 2018. Half-lives of PFOS, PFHxS and PFOA after end of exposure to contaminated drinking water. Occup. Environ. Med. 75, 46–51. https://doi.org/10.1136/oemed-2017-104651.

Lim, T.C., Wang, B., Huang, J., Deng, S., Yu, G., 2011. Emission inventory for PFOS in China: review of past methodologies and suggestions. Sci. World J. 11, 1963–1980. https://doi.org/10.1100/2011/868156.

Lin, A.Y.-C., Panchangam, S.C., Lo, C.-C., 2009. The impact of semiconductor, electronics and optoelectronic industries on downstream perfluorinated chemical contamination in Taiwanese rivers. Environ. Pollut. 157, 1365–1372. https://doi.org/10.1016/j.envpol.2008.11.033.

Mahinroosta, R., Senevirathna, L., 2020. A review of the emerging treatment technologies for PFAS contaminated soils. J. Environ. Manag. 255, 109896 https://doi.org/10.1016/j.jenvman.2019.109896.

Martin, D., Munoz, G., Mejia-Avendaño, S., Duy, S.V., Yao, Y., Volchek, K., Brown, C.E., Liu, J., Sauvé, S., 2019. Zwitterionic, cationic, and anionic perfluoroalkyl and polyfluoroalkyl substances integrated into total oxidizable precursor assay of contaminated groundwater. Talanta 195, 533–542. https://doi.org/10.1016/j.talanta.2018.11.093.

McCleaf, P., Englund, S., Östlund, A., Lindegren, K., Wiberg, K., Ahrens, L., 2017. Removal efficiency of multiple poly- and perfluoroalkyl substances (PFASs) in drinking water using granular activated carbon (GAC) and anion exchange (AE) column tests. Water Res. 120, 77–87. https://doi.org/10.1016/j.watres.2017.04.057.

Merino, N., Qu, Y., Deeb, R.A., Hawley, E.L., Hoffmann, M.R., Mahendra, S., 2016. Degradation and removal methods for perfluoroalkyl and polyfluoroalkyl substances in water. Environ. Eng. Sci. 33, 615–649. https://doi.org/10.1089/ees.2016.0233.

Miaz, L.T., Plassmann, M.M., Gyllenhammar, I., Bignert, A., Sandblom, O., Lignell, S., Glynn, A., Benskin, J.P., 2020. Temporal trends of suspect-and target-per/polyfluoroalkyl substances (PFAS), extractable organic fluorine (EOF) and total fluorine (TF) in pooled serum from first-time mothers in Uppsala, Sweden, 1996-2017. Environ. Sci. Process. Impacts 22, 1071–1083. https://doi.org/10.1039/c9em00502a.

Milley, S.A., Koch, I., Fortin, P., Archer, J., Reynolds, D., Weber, K.P., 2018. Estimating the number of airports potentially contaminated with perfluoroalkyl and polyfluoroalkyl substances from aqueous film forming foam: a Canadian example. J. Environ. Manag. 222, 122–131. https://doi.org/10.1016/j.jenvman.2018.05.028.

Möller, A., Ahrens, L., Surm, R., Westerveld, J., van der Wielen, F., Ebinghaus, R., de Voogt, P., 2010. Distribution and sources of polyfluoroalkyl substances (PFAS) in the River Rhine watershed. Environ. Pollut. Barking Essex 158, 3243–3250. https://doi.org/10.1016/j.envpol.2010.07.019, 1987.

Murakami, M., Kuroda, K., Sato, N., Fukushi, T., Takizawa, S., Takada, H., 2009. Groundwater pollution by perfluorinated surfactants in tokyo. Environ. Sci. Technol. 43, 3480–3486. https://doi.org/10.1021/es803556w.

Nickerson, A., Rodowa, A.E., Adamson, D.T., Field, J.A., Kulkarni, P.R., Kornuc, J.J., Higgins, C.P., 2021. Spatial trends of anionic, zwitterionic, and cationic PFASs at an AFFF-impacted site. Environ. Sci. Technol. 55, 313–323. https://doi.org/10.1021/acs.est.0c04473.

Ochoa-Herrera, V., Sierra-Alvarez, R., 2008. Removal of perfluorinated surfactants by sorption onto granular activated carbon, zeolite and sludge. Chemosphere 72, 1588–1593. https://doi.org/10.1016/j.chemosphere.2008.04.029.

OECD, 2018. Toward A New Comprehensive Global Database of Per- and Polyfluoroalkyl Substances (PFASs): Summary Report on Updating the OECD 2007. List of Per- and Polyfluoroalkyl Substances (PFASs) (No. ENV/JM/MONO 2018). OECD.

Pan, C.-G., Zhao, J.-L., Liu, Y.-S., Zhang, Q.-Q., Chen, Z.-F., Lai, H.-J., Peng, F.-J., Liu, S.-S., Ying, G.-G., 2014. Bioaccumulation and risk assessment of per- and polyfluoroalkyl substances in wild freshwater fish from rivers in the Pearl River

Delta region, South China. Ecotoxicol. Environ. Saf. 107, 192–199. https://doi.org/10.1016/j.ecoenv.2014.05.031.
Place, B.J., Field, J.A., 2012. Identification of novel fluorochemicals in aqueous film-forming foams used by the US military. Environ. Sci. Technol. 46, 7120–7127. https://doi.org/10.1021/es301465n.
Rich, C.D., Blaine, A.C., Hundal, L., Higgins, C.P., 2015. Bioaccumulation of perfluoroalkyl acids by earthworms (Eisenia fetida) exposed to contaminated soils. Environ. Sci. Technol. 49, 881–888. https://doi.org/10.1021/es504152d.
Ross, I., McDonough, J., Miles, J., Storch, P., Thelakkat Kochunarayanan, P., Kalve, E., Hurst, J., S Dasgupta, S., Burdick, J., 2018. A review of emerging technologies for remediation of PFASs. Remed. J. 28, 101–126. https://doi.org/10.1002/rem.21553.
Samuelsson, E.V., Thorsbrink, M., 2019. Grundvattenmagasinen Uppsalaåsen Uppsala Uppsalaåsen Fredrikslund (No. K628). Sveriges geological survey, Uppsala.
Schrenk, D., Bignami, M., Bodin, L., Chipman, J.K., del Mazo, J., Grasl-Kraupp, B., Hogstrand, C., Hoogenboom, L., Ron,), Leblanc, J., Nebbia, C.S., Nielsen, E., Ntzani, E., Petersen, A., Sand, S., Vleminckx, C., Wallace, H., Barregård, L., Ceccatelli, S., Cravedi, J., Halldorsson, T.I., Haug, L.S., Johansson, N., Knutsen, H.K., Rose, M., Roudot, A., Van Loveren, H., Vollmer, G., Mackay, K., Riolo, F., Schwerdtle, T., 2020. Risk to human health related to the presence of perfluoroalkyl substances in food. EFSA J. 18, e06223 https://doi.org/10.2903/j.efsa.2020.6223.
Schultes, L., Vestergren, R., Volkova, K., Westberg, E., Jacobson, T., Benskin, J.P., 2018. Per- and polyfluoroalkyl substances and fluorine mass balance in cosmetic products from the Swedish market: implications for environmental emissions and human exposure. Environ. Sci. Process. Impacts 20, 1680–1690. https://doi.org/10.1039/c8em00368h.
Sorengard, M., Kleja, D.B., Ahrens, L., 2019. Stabilization of per- and polyfluoroalkyl substances (PFASs) with colloidal activated carbon (PlumeStop®) as a function of soil clay and organic matter content. J. Environ. Manag. 249 https://doi.org/10.1016/j.jenvman.2019.109345.
SMHI. SMHI - vattenwebb. https://vattenwebb.smhi.se/modelarea/. (Accessed 25 April 2022).
Sörengård, M., Ahrens, L., Alygizakis, N., Jensen, P.E., Gago-Ferrero, P., 2020a. Non-target and suspect screening strategies for electrodialytic soil remediation evaluation: assessing changes in the molecular fingerprints and per- and polyfluoroalkyl substances (PFASs). J. Environ. Chem. Eng. https://doi.org/10.1016/j.jece.2020.104437, 104437.
Sörengård, M., Gago-Ferrero, P., Kleja Berggren, D., Ahrens, L., 2020b. Laboratory-scale and pilot-scale stabilization and solidification (S/S) remediation of soil contaminated with per- and polyfluoroalkyl substances (PFASs). J. Hazard Mater. 123453 https://doi.org/10.1016/j.jhazmat.2020.123453.
Sörengård, M., Kikuchi, J., Wiberg, K., Lutz, A., 2022. Spatial distribution and load of per- and polyfluoroalkyl substances (PFAS) in background soils in Sweden. Chemosphere 295, 133944. https://doi.org/10.1016/j.chemosphere.2022.133944.
Stockholm convention on persistent organic pollutants (POPS), 2018. stockholm Convention on Persistent Organic Pollutants (POPS)- Texts and Annexes - Revised In 2017. BRSMeas. http://chm.pops.int/?tabid=2511. (Accessed 25 April 2022). accessed.
Stubleski, J., Salihovic, S., Lind, L., Lind, P.M., van Bavel, B., Kärrman, A., 2016. Changes in serum levels of perfluoroalkyl substances during a 10-year follow-up period in a large population-based cohort. Environ. Int. 95, 86–92. https://doi.org/10.1016/j.envint.2016.08.002.
Swedish Food Agency. PFAS in drinking water and self-caught fish - risk management. https://www.livsmedelsverket.se/en/production-control-and-trade/drinking-water-production-and-control/t. (Accessed 25 April 2022).
Tokranov, K., LeBlanc, A.R., Pickard, D.M., Ruyle, H.J., Barber, B.B., Hull, L.B., Sunderland, R.M., Vecitis, E.D., C, 2021. Surface-water/groundwater boundaries affect seasonal PFAS concentrations and PFAA precursor transformations. Environ. Sci. Process. Impacts 23, 1893–1905. https://doi.org/10.1039/D1EM00329A.
Tröger, R., Klöckner, P., Ahrens, L., Wiberg, K., 2018. Micropollutants in drinking water from source to tap - method development and application of a multiresidue screening method. Sci. Total Environ. 627, 1404–1432. https://doi.org/10.1016/j.scitotenv.2018.01.277.
Ullberg, M., Lavonen, E., Köhler, S.J., Golovko, O., Wiberg, K., 2021. Pilot-scale removal of organic micropollutants and natural organic matter from drinking water using ozonation followed by granular activated carbon. Environ. Sci. Water Res. Technol. 7, 535–548. https://doi.org/10.1039/D0EW00933D.
Vatteninformationssytem Sverige (VISS), 2022. http://viss.lansstyrelsen.se/Waters.aspx?waterMSCD=WA46767377. (Accessed 25 April 2022) accessed.
Wang, Z., Boucher, J.M., Scheringer, M., Cousins, I.T., Hungerbühler, K., 2017. Toward a comprehensive global emission inventory of C4-C10 perfluoroalkanesulfonic acids (PFSAs) and related precursors: focus on the life cycle of C8-based products and ongoing industrial transition. Environ. Sci. Technol. 51, 4482–4493. https://doi.org/10.1021/acs.est.6b06191.
Winquist, G., 1992. The Structures and Development of the Uppsala Infiltration Projekt, ISBN 91-7388-003-5.
Zhang, R., Yan, W., Jing, C., 2014. Mechanistic study of PFOS adsorption on kaolinite and montmorillonite. Colloids Surf. A Physicochem. Eng. Asp. 462, 252–258. https://doi.org/10.1016/j.colsurfa.2014.09.019.